Electromagnetic Levitation System : An Experimental Approach

H. D. Taghirad, M. Abrishamchian, R. Ghabcheloo
K. N. Toosi University of Technology
Department of Electrical Engineering
Tehran, Iran

Abstract— **In this paper, we propose a simple method for controlling an electromagnetic levitation (*Maglev*) system. The model of the Maglev system under consideration in this paper is third order, inherently nonlinear and unstable. For designing a controller to obtain a good disturbance rejection and being insensitive to parameter variations, we use an inner-loop and an outer-loop configuration. The configuration is the key to solve this problem. By using a nonlinear state transformation in the feedback path, a cascaded PI controller and a redefined input in the inner loop, we obtain a linear second order system. Furthermore, to achieve a stable system with a good disturbance rejection, we design a PID controller cascaded with the inner loop system in the negative unity feedback configuration in the outer loop. We show that the closed-loop system is robustly stabilized against the mass variation. Simulation results show that despite actuator saturation limits, the performance of our simple structure controller is comparable to that reported in the literature. In order to assess these results in practice, an experimental setup is designed and being constructed. The simulation analysis is based on the parameters of this experimental setup.**

Keywords— **Magnetic levitation system, Suspension system, Feedback linearization, PID, Nonlinear system, Robustness.**

I. Introduction

One of the ways that non-contact surfaces are maintained is via magnetic suspension. This system is commonly referred to as Magnetically Levitated system (*Maglev*) which has been used in the vehicle suspension system and magnetic bearing system by B. A. Holes of university of Virginia in 1937 for the first time; in 1954, this system was utilized by Laurencean and Tournier at ORENA in France for the purpose of aerodynamic testing in wind tunnels [1]. Furthermore, the system is being used in many other applications such as magnetic suspension high speed trains [2].
The electromagnetic suspension systems (EMS systems) can be divided into two types; see [3]

- Repulsion type
  In this type of the electromagnetic suspension system, suspended part(such as train) repulses the fix part(such as rail). This type is realizable with materials of permeability (μ_r) less than unity (diamagnetic material) and with superconductors with ($\mu_r = 0$). A disadvantage of this type of suspension systems is that an auxiliary wheeling suspension is needed for operation below the critical speed (typically $80Km/h$) specially at zero speed, i.e., when the suspended object is stationary. These systems are naturally stable with small damping ratio.
- Attraction type
  In this type suspended part(such as train) attracts the fix part(such as rail). Realization of this type is possible by ferromagnetic and/or permanent magnet. This type of EMS system has one significant advantage in that it provides attraction force at zero speed, but such a system is inherently unstable.

The increasing use of the Maglev technology in its various forms has resulted in active research in this area. The electromagnetic suspension technology has already been applied to magnetically levitated carriers [4], magnetic bearings [5], and vibration isolators [6]. Hence, some advanced theories are utilized to get better performance, such as, H_∞ control [7], μ-synthesis [8] and feedback linearizing control law [9].

In this paper we will summarize the mathematical model of the system that is taken from [3], which is elaborated in Section II. In Section III, we design a controller that achieve our objectives.

In this controller, we consider a state transformation followed by a PI controller in the inner loop that satisfies the necessary performance characteristics for the actuator. Next we design a PID controller that stabilizes the whole system and discuss the robustness of the closed-loop system against mass variations. The foundation of the implementation including some details of mathematical design and data acquisition system is the subject of Section IV. In Section V, some issues that required to be addressed for proper simulation of the model are discussed and also simulation results are presented. In Section VI, we provide a comparison between the performance of the proposed controller and a feedback linearizing controller for stabilizing and commanding the EMS system which has been proposed in [9]. Finally conclusions are summarized.

II. **Mathematical Model**

To synthesize a feedback control system, a relatively precise model of the plant is required. It is known that a mathematical model cannot fully express the behavior of the real physical plant. An ideal mathematical model has various uncertainties such as parameter identification errors, unmodeled dynamics and neglected nonlinearities. The controller is required to have robust stability and performance in presence of such uncertainties in the model and also due to bounded disturbance.

Crude simulation studies do not reveal all the practical pitfalls of a real system. Therefore, more realistic mathematical model which includes all different aspects of the system behavior is needed to give us a better knowledge in constructing a *Maglev* system. We use the model that is given by [3].

In the model as shown in Figure 1, the instantaneous flux linkage between the two magnetized bodies through the air gap $z(t)$ is ϕ_m. If the leakage flux is ignored, that is $\phi_t = \phi_m$, then

$$L(z) = \frac{\mu_0 N^2 A}{2z(t)} \tag{1}$$

where μ_0 is vacuum permeability, N is the number of turns of the magnet winding, and A is pole face area. Furthermore, note that the inductance L varies with changes in the air gap. Also the attraction force at any instant of time is given by,

$$F(i,z) = \frac{\mu_0 N^2 A}{4}\left(\frac{i(t)}{z(t)}\right)^2 \tag{2}$$

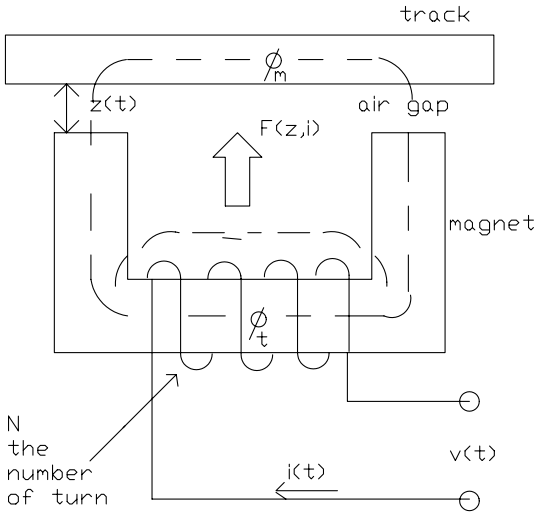

Fig. 1. Schematic of an electromagnetic suspension system

Thus if the total resistance of the circuit is denoted by R, then the instaneous voltage $v(t)$ (across the magnet winding) controlling the excitation current $i(t)$ is given by

$$v(t) = Ri(t) + \frac{\mu_0 N^2 A}{2z(t)}\frac{di(t)}{dt} - \frac{\mu_0 N^2 A i(t)}{2z(t)^2}\frac{dz(t)}{dt}. \tag{3}$$

Note a varying inductance with respect to $z(t)$ in the second term, and that the third term denotes a voltage which varies with changes in the air gap $z(t)$ and its rate of change similar to back EMF voltage introduced in a DC motor. This expression displays the actuator dynamic (electrical plant).

We now give the vertical dynamic of the system by the following equation,

$$m\ddot{z}(t) = -F(i,z) + mg + f_d(t) \tag{4}$$

where $f_d(t)$ is disturbance force input and m is the suspended object mass. This equation describes the dynamics of the plant (mechanical plant). The foregoing EMS system can be rewritten in the following equations:

$$\dot{x}_1 = x_2 \tag{5}$$

$$\dot{x}_2 = -\frac{k}{2m}\left(\frac{x_3}{x_1}\right)^2 + g + \frac{1}{m}f_d \tag{6}$$

$$\dot{x}_3 = -\frac{R}{k}x_1 x_3 + \frac{x_2 x_3}{x_1} + \frac{1}{k}x_1 u(t) \tag{7}$$

$$y = x_1 \tag{8}$$

where y is output, $x_1 = z$ (vertical air gap) [m], $x_2 = \dot{z}$ (vertical relative velocity) [m/s], $x_3 = i$ (magnet current) [A], $g = 9.8$ [m/s^2] and $k =$

$\frac{\mu_0 N^2 A}{2}$ (force factor).
Equations (1), (2) and (3) are valid when the magnetized core is not working in saturation region and also when the air gap clearance, $z(t)$, is not too small. Therefore, state-space Equations (5), (6), (7) and (8) for an EMS system are valid in these conditions. We have considered them in our experimental setup design. To concern the limited permability and leakage, we should add a bias to x_1 (in constructed set up is about 0.2mm).

III. Control System Design

Electromagnetic suspension system is essentially an unstable system due to inverse force-distance characteristic, see Equation (2). From Equations (3) and (4), it is obvious that the system dynamics consists of two parts, actuator dynamic (electrical part), and plant dynamics (mechanical part). These two subsystem are strongly coupled because distance of suspended object from the magnet $z(t)$ influences the magnet inductance, see Equation (1).
We can reduce the effects of two parts by a simple state transformation of $x = x_3/x_1$. Then the new state equation for the plant dynamics become

$$\dot{x}_1 = x_2 \tag{9}$$

$$\dot{x}_2 = -\frac{k}{2m}x^2 + g + \frac{1}{m}f_d \tag{10}$$

and for actuator dynamics, we have

$$\dot{x} = -\frac{R}{k}x_1 x + \frac{1}{k}u(t) \tag{11}$$

We now consider the control synthesis for the actuator system. Let's view the actuator dynamic differently. Rewrite Equation (11) for input u and output x and consider the term $-\frac{R}{k}x_1$ as an uncertainty. Here,

$$\dot{x} + a(t)x = \frac{1}{k}u \tag{12}$$

where $a(t) = \frac{R}{k}x_1$ represents the uncertainty. Since x_1 is a mechanical variable, it varies much slower than an electrical variable x, provided the closed-loop actuator has high-bandwidth. We propose that by choosing a high gain PI controller, we can achieve a high bandwidth actuator inspite of the variation of $a(t)$. Consider,

$$u = k_o K_p e + k_o K_i \int_0^t e dt \tag{13}$$

where $e = x_d - x$, x_d is desired value of the x, and k_o is a given value of k. By substitution of u in the Equation (12), we have

$$\dot{x} + ax = K_p e + K_i \int_0^t e dt \tag{14}$$

After some manipulations, for a step input x_d, we achieve the following dynamics for error,

$$\ddot{e} + (K_p + a)\dot{e} + (K_i + \dot{a})e = x_d \dot{a}. \tag{15}$$

By considering the following Lyapunov function and its derivative, we find conditions for stability:

$$\begin{aligned} V(x,t) &= \frac{1}{2}(\dot{e} + a(t)e)^2 + \frac{1}{2}(K_i + a(t)K_p)^2 \\ \dot{V} &= -K_p\dot{e}^2 - (K_i a - \frac{1}{2}\dot{a})e^2 \end{aligned} \tag{16}$$

The dynamics (15) is robustly stable and the error goes to zero if following two conditions are satisfied: $\dot{V} < 0$ or equivalently K_i, $K_p > 0$, $\frac{K_i}{K_p} > \max_t \frac{\dot{a}(t)}{2a(t)}$ and $\lim_{t\to\infty} \dot{a} = 0$. Indeed by choosing K_i high enough, we satisfy first condition and the second condition is satisfied if the whole closed-loop is stabilized. By choosing high gains K_i and K_p such that the actuator has large bandwidth, the actuator dynamics can be neglected. Hence x can be considered as the input for plant dynamics. Considering x^2 as the input to the plant dynamics and rewriting Equations (9) and (10) with $u = x^2$, the model is simplified to

$$\ddot{x}_1 = -\frac{k}{2m}u + g + \frac{1}{m}f_d. \tag{17}$$

We now consider designing a controller such that the closed-loop system achieve the following objectives:

1. Robust stability of the closed-loop system against mass variation.
2. Good disturbance attenuation performance.
3. Non-negative control action, u.

We can achieve all these objectives with a PID controller. The integral term makes the system a type-1 system to assure zero steady-state error. The proportional and derivative gains are selected such that to guarantee the robust stability of the system. The whole closed-loop system is shown in Figure 5 in Section V.

IV. Experimental Setup

A. Experimental Configuration

In order to examine the proposed control law in practice, and to obtain a more realistic estimate of the practical challenges of EMS system,

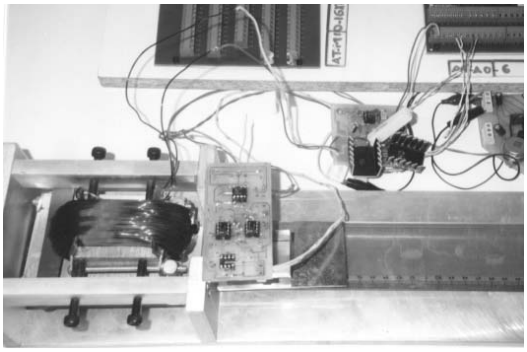

Fig. 2. A scanned photo of the constructed setup

an experimental setup of this system is designed and being constructed. Figure 3 illustrates the block diagram of the constructed system. In this figure it is shown that to provide more flexibility and simplicity to the hardware, all the blocks in the dashed-line box are implemented through software. In order to do that, the setup is equipped with an IBM-PC (Pentium 133 MHz) and a National Instruments data acquisition and conditioning card (NIDAQ: AT-MIO-16X-50).

Figure 2 illustrates a photo of the experimental setup. The mechanical setup consists of a U-shape magnet and a rail-shape track to simulate the inherent application of magnetic suspension trains. We choose a laminated and U-shape magnet to reduce the eddy current and hysteresis effects [3]. The suspended object motion is concentrated by a long flexible beam to be free only in one direction [10]. By some corrections in the parameters, we can assume that the track travels approximately only in the vertical direction. The total accessible range of the travel is approximately between 0.5 to $5mm$.

In order to measure the air gap clearance, we tried sensors which are commercially available. However their linearity and range of application

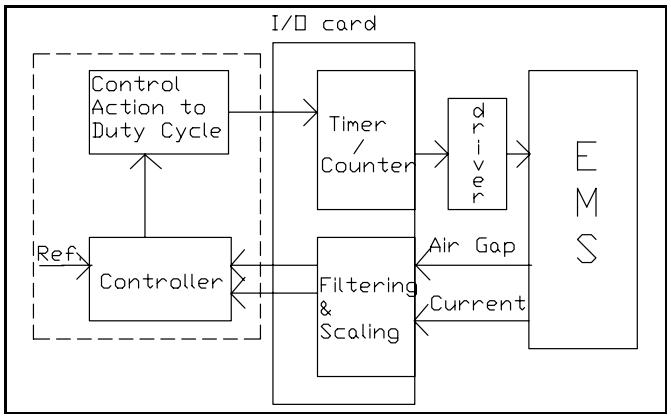

Fig. 3. Block diagram of the experimental setup

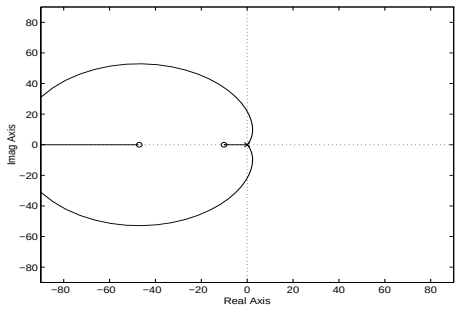

Fig. 4. Root locus of the mechanical plant

dose not match our requirements. Therefore, we have designed and have constructed a custom made capacitive transducer for this purpose. The sensor consists of a rectangular plate surrounded by a thin border as a guard to reduce the electromagnetic noise effect. The capacitance is demodulated to a voltage directly proportional to air gap that is approximately linear in the accessible range. The current is measured using a small resistor cascaded with the electromagnetic coil. The power source is designed using a PWM type voltage chopper with DC link voltage of 24 volts, which are considered in the simulations as to be described in Section V. All inputs and output are decoupled from NIDAQ card by optocouplers. The setup components are individually tested and calibrated and open-loop experiments are conducted to verify the integrability of the whole setup. Closed-loop experiments are underway.

B. Derivation of Model and Controller

After the construction of the setup, the nominal parameters of the experimental setup are estimated and given in Table 1 (All parameters in the table and in this section are in SI units.) For these parameters and nominal air gap, $z_o = 2.5$mm, we can find a_o from Equation (12) as $a_o = 75$. To achieve a high bandwidth closed-loop system with $\omega_n = 500$ and $\xi = 1$, we choose PI controller as $K_p = 1000$, $K_i = 250000$. And also for the PID controller considering mass uncertainty we choose controller gains as follows to assure robust stability,

$K_p' = 12 \times 10^3 \frac{2m_o}{k_o}$,

$K_i' = 100 \times 10^3 \frac{2m_o}{k_o}$ and

$K_d' = 0.21 \times 10^3 \frac{2m_o}{k_o}$.

where m_o and k_o denote nominal values of m and k, respectively. By this choice the closed-loop plant dynamics has its roots at -10, -100 and -100 in the nominal condition. Let's choose the root locus gain as $k_m = \frac{k}{2m} \times \frac{2m_o}{k_o}$, it means in

the nominal condition we have $k_{m_o} = 1$. The root locus of the closed-loop plant dynamics is shown with respect to variation of the factor k_m in Figure 4. The whole system is stable for large values of k_m and also for small values down to $k_m = 3.46 \times 10^{-2}$. Therefore, closed-loop system is very robust against mass and force factor variation. This fact is verified in the following section via simulation.

V. **Simulation Results**

For simulation, we use simulink toolbox of MATLAB as shown in Figure 5. Since this simulation is done to check the feasibility of the controller in practice, we consider the following points in the simulation:

1. We use the square root of the absolute value of the output to avoid the failure of simulation because of negative values of the controller output. But, we note that the state x in the actuator dynamics would not be physically meaningful to allow negative values.
2. We model hard stops in mechanical setup as very stiff springs to avoid the discontinuity in the equation of motion of the plant and the numerical difficulties of integrating them. In this method when the track is passing through the limits as

$$\begin{aligned} if \quad x &> x_{sat} \\ F_{sat} &= k(x - x_{sat}) \\ \vdots & \quad \vdots \\ \dot{x}_2 &= -\frac{k}{2m}\left(\frac{x_3}{x_1}\right)^2 + g + \frac{1}{m}(f_d + F_{sat}) \end{aligned}$$

3. One of important practical limits of the controller implementation is the bounded control effort we can provide in practice. To visualize this limit, a simulation block is added which illustrates the required voltages and their limit of $0 - 24$ volts.

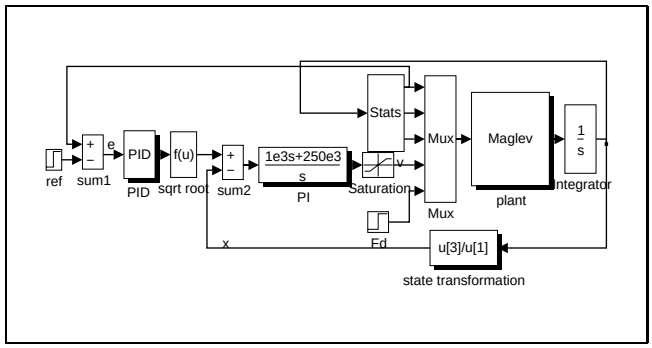

Fig. 5. Closed-loop system in simulink

4. PID controller can only be implemented approximately in practice. The effect of this approximation considered by using approximate PID controller box of simulink.

The effects of variations in mass and also disturbance attenuation of closed-loop system are shown in corresponding figures as explained in the following section.

VI. **Comparison with Feedback Linearizing Controller**

A nonlinear feedback linearizing controller is reported in [9]. Behaviors of our controller and the feedback linearizing controller are compared in Figures 6 and 7. In these figures, dash-dot curves correspond to the feedback linearizing control and our proposed control is shown by solid curves. Below each figure, the experiment conditions including transient behavior and disturbance rejection of the nominal and disturbed plants are mentioned. Figure 6 shows the transient response of the system, (a) with nominal mass $m = 3.3$, and (b) with $m = 16.5$. One can see that the response of the feedback linearizing controller is a bit better than ours in case of nominal mass (Figure 6-a), but has steady-state error in perturbed conditions (Figure 6-b), while the response of the proposed controller approaches the desired value. Their behaviors in response to the disturbance force is depicted in Figures 7. Our proposed controller has larger overshoot but the output reaches the desired value. We note that the feedback linearizing control reported in [9] needs an extra sensor to measure the rate of the air gap variations, but performance is not much better than our proposed controller.

VII. **Conclusions**

This paper presents a new method for controlling the electromagnetic suspension system as a 1-DOF system. By a state transformation the complex nonlinearities and the coupling between the plant and the actuator are reduced, each subdynamics are controlled separately as reported for DC motor control [11]. With this difference that in the motor control, the inner loop path feeds back just current, while because of dynamic of the EMS system, we choose current divided by the air gap as the feedback. PI and PID controllers are designed to satisfy our objectives, and their performance is compared to some methods reported in the literature. It is concluded that, in spite of

TABLE I

THE NOM INAL PARAMETERS OF EXPERIMENTAL SETUP

Description	Notation	Value
Track mass	m	3.3
Number of turns	N	565
Pole face area	A	78.6×10^{-5}
Total resistance	R	1.5
Force factor	k	5×10^{-5}
Nominal gap	z_o	2.5×10^{-3}

simple shape of controller, good performances are achievable.

REFERENCES

[1] E. E. Covert, "Magnetic Suspension and Balance Systems," *IEEE AES Magazine*, pp. 14–22, May 1988.

[2] A. R. Eastham and W. F. Hayes, "Maglev Systems Development Status," *IEEE AES Magazine*, pp. 21–30, January 1988.

[3] P. K. Sinha, *Electromagnetic Suspension, Dynamics and Control*. IEE control engineering series, 1987.

[4] M. Morishita et al, "A New Maglev System for Magnetically Levitated Carrier System," *IEEE Transactions on Vehicular Technology*, vol. 38, pp. 230–236, November 1989.

[5] A. M. Mohamed and I. Busch-Vishniac, "Imbalance Compensation and Automation Balancing in Magnetic Bearing Systems Using the Q-parameterization Theory," *IEEE Transactions on Control System Technology*, vol. 3, pp. 202–211, June 1995.

[6] K. Watanabe et al, "Combination of H_∞ and PI Control for an Electromagnetically Levitated Vibration Isolation System," in *Proceedings of the 35st Conference on Decision and Control*, pp. 1223–1228, 1996.

[7] F. Zhang and K. Suyama, "H_∞ Control of Magnetic Suspension System," in *Proceedings of the 33st Conference on Decision and Control*, pp. 605–610, 1994.

[8] M. Fujita et al, "μ-Synthesis of an Electromagnetic Suspension System," *IEEE Transactions on Automatic Control*, vol. 40, pp. 530–536, March 1995.

[9] S. Joo and J. M. Seo, "Design and Analysis of the Nonlinear Feedback Linearizing Control for an Electromagnetic Suspension System," *IEEE Transactions on Control System Technology*, vol. 5, pp. 135–144, January 1997.

[10] D. L. Trumper, S. M. Olson, and P. K. Subrahmanyan, "Linearizing Control of Magnetic Suspension Systems," *IEEE Transactions on Control System Technology*, vol. 5, pp. 427–438, July 1997.

[11] P. R. Be'langer, *Control Engineering : A Modern Approch*. Saunders College, 1995.

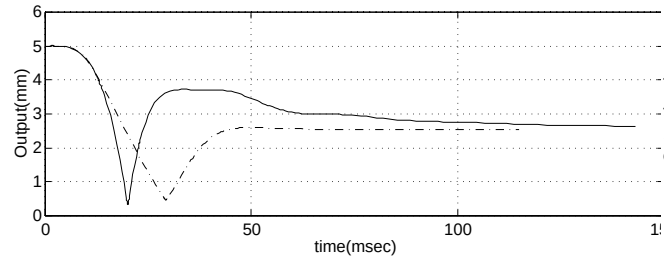

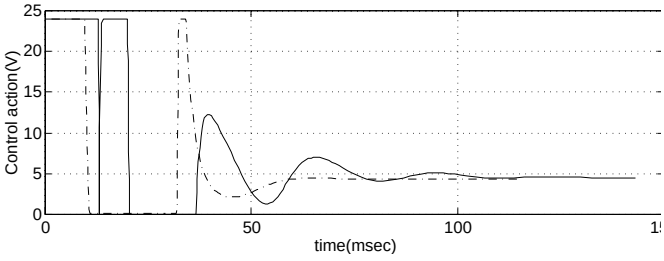

(a)

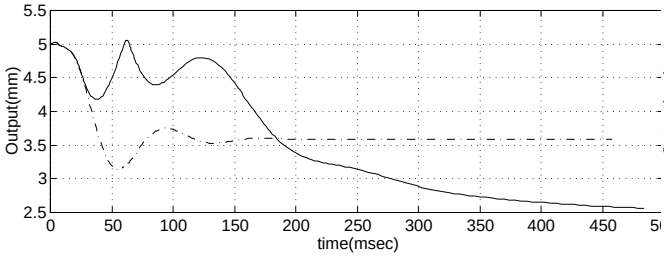

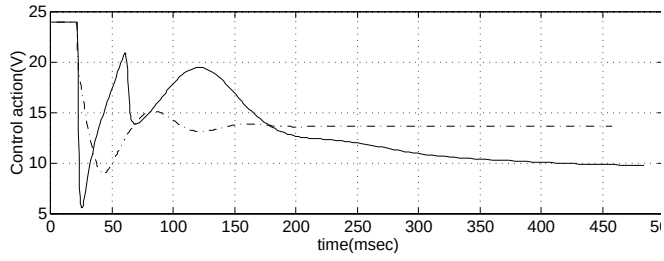

(b)

Fig. 6. Transient response in traveling from 5mm to 2.5mm of (a) the nominal system (m = 3.3 Kg) and (b) perturbed system (m = 16.5 Kg). Solid: proposed controller, dash-dot: feedback linearizing controller

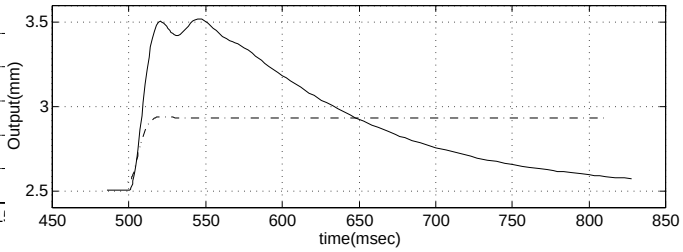

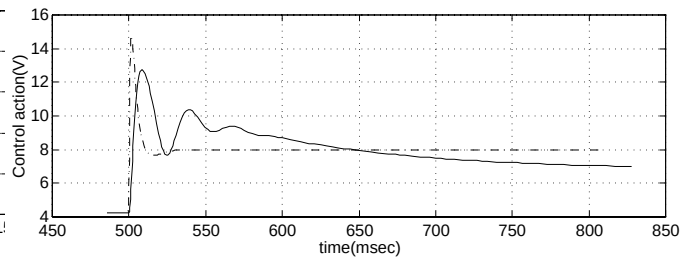

(a)

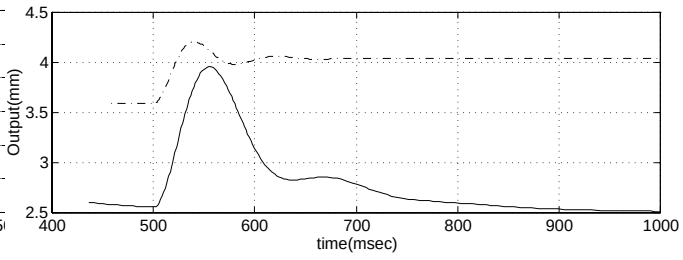

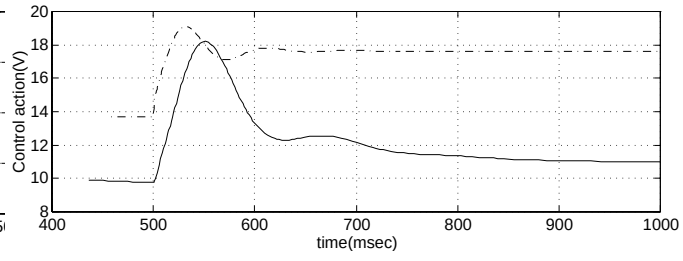

(b)

Fig. 7. Response to disturbance force of f_d = 50 N of (a) the nominal system (m = 3.3 Kg) and (b) perturbed system (m = 16.5 Kg). Solid: proposed controller, dash-dot: feedback linearizing controller